ELSEVIER

Chlorinated alumina as an alkylation catalyst: influence of superficial HCl

G. Clet [a], J.M. Goupil [a], G. Szabo [b], D. Cornet [a,*]

[a] *Laboratoire Catalyse et Spectrochimie, UMR CNRS 6506, ISMRA, Université de Caen, 6, Bd du Maréchal Juin, 14050 Caen, France*
[b] *Centre Européen de Recherches et Techniques TOTAL, 76700 Harfleur, France*

Abstract

Chlorinated alumina catalysts were obtained by reacting gamma-alumina with gaseous CCl_4 or hydrogen chloride under various conditions. They had chlorine contents between 4 and 6% by weight, and differed in surface acidity. They were tested as catalysts for the alkylation of isobutane with 2-butene using a fixed bed plug flow reactor. Alumina reacted with CCl_4 was found inefficient for this reaction. However, the solid chlorinated with HCl above 800 K was able to catalyze alkylation at a temperature as low as 273 K. Moreover, the CCl_4-reacted solid could be activated upon further treatment with HCl at moderate temperatures (370 to 550 K). However, the catalytic activity decays after a few hours on stream. The composition of the alkylate varied somewhat with time on stream: large amounts of cracked products appeared during the initial period, after which the selectivity to trimethylpentanes (TMP) was comparable to that of other solid catalysts. The presence of hydrogen chloride bound to the catalyst surface was established by measuring the temperature-programmed desorption (TPD) of HCl from the various Al_2O_3–Cl. For the active catalysts, desorption started at temperatures (350–400 K) well under those for the CCl_4-treated sample, but all solids continuously released HCl above 650 K. Thus, HCl interacts with particular Lewis acid sites of Al_2O_3–Cl, and creates the strong Brønsted sites required for catalytic alkylation. © 1999 Elsevier Science B.V. All rights reserved.

Keywords: Isobutane alkylation; Butene; Chlorinated alumina; Temperature-programmed desorption; Acidity

1. Introduction

Recent specifications on gasoline formulation lead to an increased demand for trimethylpentanes (TMP), which are obtained by reacting isobutane with butene. Alkylation is currently performed in the liquid phase, with H_2SO_4 or HF as catalysts. Full conversion of the alkene occurs at dilution 10–20, with more than 60%

selectivity to TMP [1–3]. However, solid catalysts are actively sought to replace the liquid acids that are potentially dangerous [4].

Various solids featuring Brønsted acid sites have been proposed as alkylation catalysts, notably zeolites [5,6], sulfated zirconia [7], supported heteropolyanions [8] or protonic acids immobilized on solid oxides [9,10]. But all of these deactivate more or less rapidly [11]. Lewis acids supported on oxides, such as BF_3/SiO_2, have also been patented as alkylation catalyst

---

* Corresponding author. Fax: +33-31-452822

[12]. Chlorinated alumina, which has been mentioned for this purpose, apparently belongs to the same class, as the reaction of alumina with CCl_4 [13] and then eventually with $AlCl_3$ [14] is likely to impart Lewis acidity to the solid.

However, the $AlCl_3 + HCl$ mixture was reported earlier to be an efficient catalyst in the liquid phase alkylation of isobutane by several alkenes [15], so that Brønsted acidity may be involved in the process. Indeed, the isobutane–butene alkylation presents an opportunity to investigate the surface acidity of Al_2O_3–Cl. In this study, catalysts obtained through different chlorinating procedures will be compared for the isobutane–butene alkylation. The amount of HCl bound on each solid will be measured by temperature-programmed desorption (TPD), to determine the influence of the bound HCl upon activity. The TPD results will then be compared with those obtained in an infrared study using adsorbed bases [16].

2. Experimental

2.1. Catalyst preparation and activation

The starting material was a γ-alumina from AKZO (Ketjen CK-300) with BET area 195 m^2 g^{-1}, pore volume 0.42 cm^3 g^{-1} and average pore diameter 8 nm. The small cylindrical pellets were about 3.8 mm long and 1.65 mm in diameter. This solid was previously dehydrated at 673 K, unless otherwise stated. Chlorination was then carried out at atmospheric pressure by reacting 1 g of pellets with a gas flow containing the selected chlorine compound, generally for 1 h. The reagents, the experimental conditions and the catalysts names are listed in Table 1.

The chlorination with CCl_4 diluted in N_2 proceeded at 548 K (catalyst termed G). For the direct chlorination with HCl [17], alumina was first dehydrated at 813 K, and then chlorinated at 943 K with some hydrogen added to HCl (catalyst termed P). A third method involved the reaction of alumina with CCl_4–N_2 first, and then with HCl–H_2, both at 548 K (catalyst termed S).

The cooling procedure following chlorination proved to be important. Catalysts G were flushed 1 h more with dry nitrogen at 573 K, then cooled to ambient. Those treated with HCl (catalysts P or S) were quickly cooled down to 353 K under a reduced flow of HCl + H_2 mixed with N_2, and then briefly purged with N_2. All catalysts were finally transferred to the reactor or to the TPD system under dry N_2.

When examined by X-ray diffraction, the structure of alumina did not appear modified upon chlorination. Nitrogen sorption measurements showed that the surface area of alumina had decreased by 10% upon treatments G or S. For sample P, the area decreased by 24% and the average pore diameter rose from 8 to 12 nm.

2.2. Catalytic measurements

The tube containing 1 g of the chlorinated catalyst was inserted in a cylindrical steel reac-

Table 1
Experimental conditions for alumina chlorination

Catalyst	Dehydration temperature (K)	Reagent	Reaction temperature (K)	Gas flow rate (cm^3 min^{-1})	Purge temperature (K)	Cl content (wt.%)
G	673	CCl_4–N_2 (1–12)	548	10	573	5.9
P	813	HCl–H_2 (4–1)	943	30	353	4.3
S	673	CCl_4–N_2 (1–12)	548	10		6.5
		then HCl–H_2 (4–1)	548	30	353	

tor, working in the fixed bed mode as previously described [18]. The pressure was set at 1.5 MPa by means of a relief valve. Before each run, the reactor containing the catalyst was pressurized with nitrogen and the temperature set at the desired value, usually 273 K. The liquid feed of isobutane and *trans*-2-butene (mole ratio 20:1) was then introduced through a metering pump at a rate of 0.23 ml min^{-1}. Most of the alkylation runs were performed at 273 K, with a specific mass flow rate of butene equal to 0.35 g h^{-1} (g cat)$^{-1}$.

About 50 min after the pump was started, the liquid had filled up the reactor section, and the reacted mixture vaporized through the relief valve. It took some more time for the exit gas to reach its nominal flow rate. At that time (t_0, usually 90 min), a first gaseous sample was collected for analysis by gas chromatography (GC) using a CPSIL-5A capillary column. Analyses were repeated at 45-min intervals. The reaction products were grouped as light products (C_5–C_7), octanes and heavy products (C_9–C_{11}).

2.3. TPD measurements

The amount of HCl that could be released from the Al_2O_3–Cl catalysts was determined by TPD. The flow of dry helium being set at 25 cm^3 min^{-1}, the temperature was raised from 313 to 973 K at a constant rate of 2.5° min^{-1}. The residual water content in the He carrier gas was controlled by means of a Panametrics gauge: it was < 5 ppm.

The effluent gas bubbled in a dilute sodium hydroxide solution, and the H$^+$ ions appearing in the solution were titrated at all times by automatic addition of M/10 base. The total amount of chloride ions in the solution at the end of the TPD was titrated by Ag$^+$: the result accurately matched the cumulated H$^+$. The amounts of chlorine on the solid before and after the TPD were determined by chemical analysis.

3. Results and interpretation

3.1. Catalytic activity: influence of the chlorination procedure

3.1.1. Alumina chlorinated by CCl$_4$

A previous work had shown that alumina CK-300 chlorinated by CCl$_4$ at 548 K (catalyst G) could catalyze the alkylation of isobutane with ethylene [18]. At 273 K and ethylene dilution $\alpha = 20$, ethylene was fully converted during the first 50 h on stream, and 85% of the alkylate consisted of branched hexanes resulting from a simple alkylation.

The same catalyst G is found inactive for the alkylation with 2-butene under similar conditions, as the conversion of butene is only 3% at the first analysis, and decreases to zero after 2 h on stream (Fig. 1). Similarly, alumina samples differing in origin or in surface area, and chlorinated by CCl$_4$, appeared inactive. Furthermore, when alumina CK-300 was chlorinated with C_2Cl_6 in place of CCl$_4$, the solid was again inactive in alkylation with butene, although it was found active in the reaction with ethylene [19].

Therefore, alumina chlorinated with CCl$_4$ or similar molecules is unable to catalyze the alkylation with butene. This is rather unexpected,
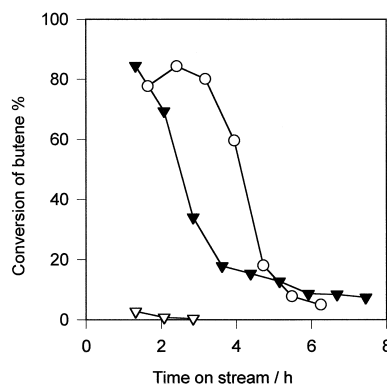

Fig. 1. Alkylation of isobutane with butene over several Al_2O_3–Cl at 273 K. Conversion of butene as a function of time on stream. Dilution $\alpha = 20$ mol mol^{-1}. Butene mass flow rate 0.35 g g^{-1} h^{-1}. (○) Catalyst P. (▽) Catalyst G. (▼) Catalyst S.

since butene is intrinsically more reactive than ethylene. Thus, over the Lewis catalyst G, polymerization of butene (or repeated alkylations) occurs more rapidly than product desorption so that, after a few minutes, the sites are completely blocked by tightly bound species. With ethylene, the inhibition is more moderate and alkylation reaches a steady-state level. Hence, a different type of surface acidity was sought by changing the mode of chlorination of alumina.

3.1.2. Alumina chlorinated with HCl

Hydrogen chloride is known to react with the surface of alumina at 600 to 1000 K [17]. Spectroscopic studies indicate that the hydroxyl groups are first substituted by Cl atoms. Then in a second stage, some more HCl dissociates upon Al–O sites with creation of new OH groups bearing Brønsted acidity [20]. Al_2O_3–Cl catalysts obtained in this way contain less chlorine than those reacted with CCl_4 (4.3% vs. 5.9%, see Table 1) but turn out to be active for the isobutane–butene alkylation, best results being obtained after reaction with HCl + H_2 at 943 K (Catalyst P).

Fig. 1 shows the course of a reaction with this catalyst P in the same conditions as before ($T = 273$ K, dilution $\alpha = 20$). The butene conversion was 78% at the first analysis, and rose to 82% at the next one. The fact that the recorded conversion never reached 100% was probably due to a partial but transient retention of the C_8 and heavier products when the solid was contacted with the isobutane–butene feed at 273 K. This gave the appearance of rather stable activity during the first 3 h. However, after 3 to 4 h on stream, the conversion decreased very rapidly.

The alkylate contained exclusively branched alkanes with five or more carbons. As with other solid catalysts [21,22], the composition strongly varied with time on stream (Fig. 2). Initially, the major products were the C_5–C_7 (50%), with only 44% octanes and 6% heavy products C_{9+}. With the increase of TOS, the octanes rose to 77% while the light products
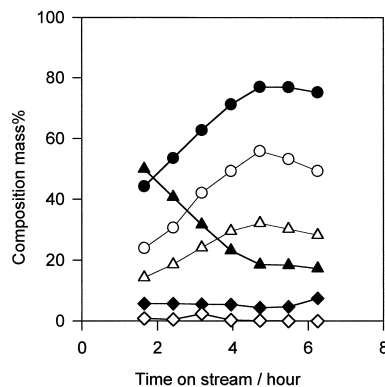
Fig. 2. Alkylation of isobutane with butene over Al_2O_3–Cl (catalyst P) at 273 K. Composition of the alkylate (mass%) as a function of time on stream. (▲) Light products. (♦) Heavy products. (●) Octanes. (○) TMP. (△) 2,2,4-TMP. (◇) 2,2,3-TMP.

decreased to 20%. The detailed product distribution will be presented later on.

Thus, catalyst P chlorinated with HCl at 943 K shows a high initial activity in alkylation with butene at a temperature as low as 273 K. However, the conversion measured in a fixed bed reactor declines after a few hours. An alternative method of preparation involving milder treatments was then sought.

3.1.3. Catalysts chlorinated in two steps

Alumina chlorinated with CCl_4 was shown to become more efficient in hydrocarbon conversion when HCl was added to the reactant feed [19,23]. Hence, a possible way to convert the solid G (reacted with CCl_4) into an active alkylation catalyst consists in a further treatment with HCl at moderate temperature. Best results were obtained when catalyst G was flushed with HCl + H_2 at temperatures above 373 K, preferably 548 K. The final catalyst S contained more chlorine (6.5%) than solids G and P (Table 1).

The initial conversion of butene over catalyst S was 85%, slightly above that of catalyst P (Fig. 1). However, conversion did not go through a maximum with time, and decayed faster than with P. Again, the alkylate contained exclusively alkanes, whose composition changed with catalyst age in the manner shown in Fig. 3. At the first analysis, the cracked products C_5–C_7

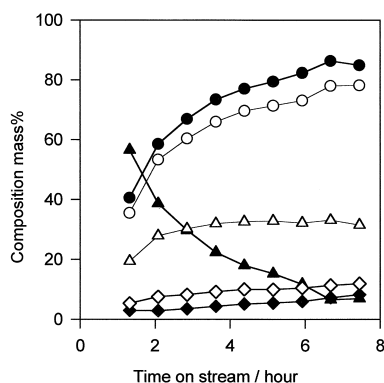Fig. 3. Alkylation of isobutane with butene over Al_2O_3–Cl (catalyst S) at 273 K. Composition of the alkylate (mass%) as a function of time on stream. (▲) Light products. (◆) Heavy products. (●) Octanes. (○) TMP. (△) 2,2,4-TMP. (◇) 2,2,3-TMP.

amounted to 56%, the octanes to 41%, and heavy products to 3%. When TOS increased, the proportion of light products over catalyst S decreased faster than with P, and the octanes increased more rapidly, to reach a higher final level.

3.1.4. Catalysts P and S: compared product distributions

The different alkylate compositions observed with the chlorinated catalysts P and S prove that these are not equivalent. Reactions were run at a fixed flow rate during catalyst deactivation, so that selectivities may be compared at equivalent conversions. Therefore, the percentages of butene converted to TMP, DMH, light or heavy products are plotted on Fig. 4 vs. overall butene

conversion. During the early period, catalyst P produced slightly more octanes than S at an equivalent conversion. Then as conversion decreased, the yields of octanes became similar on both catalysts. However, the proportion of TMP in the C_8 was lower with catalyst P, varying from 54% to 73% with increasing TOS, while it remained nearly constant at 90% with catalyst S (Table 2). As the selectivity to C_8 improved with catalyst age, the alkylate contained about 20% DMH at all times over solid P, and much less with S.

Typical repartitions of the TMP isomers appear in Table 2. Catalyst P gave a near constant proportion (60%) of the thermodynamically favored 2,2,4-TMP and very little 2,2,3-TMP (under 5%). Over catalyst S, the 2,2,4-TMP decreased from 54 to 40% when the conversion dropped from 85 to 7%, but 15% of 2,2,3-TMP were found at all times. Hence, although the primary alkylation with 2-butene reads:

$$n\text{-}C_4H_8 + t\text{-butyl}^+ \rightarrow 2,2,3\text{-TMP}^+ \quad (a),$$

the 2,2,3-TMP$^+$ carbenium ion rapidly isomerizes to other TMP$^+$, as methyl shift runs faster than desorption by hydride transfer:

$$TMP^+ + i\text{-}C_4H_{10} \rightarrow TMP + t\text{-butyl}^+ \quad (d).$$

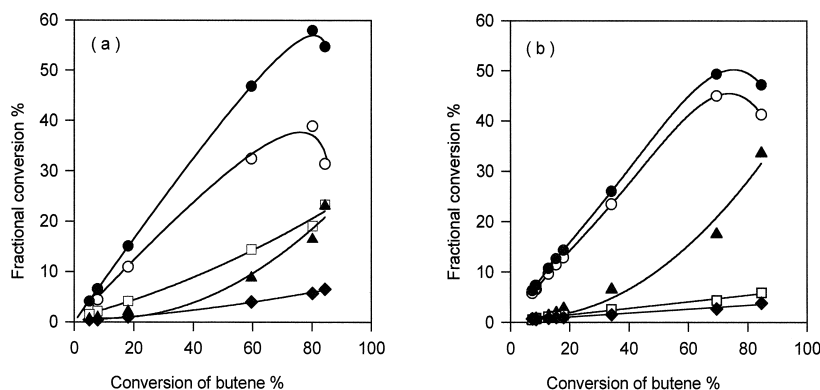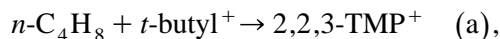The TMP distributions indicate that step (d) occurs faster on catalyst S than on P.

Fig. 4. Selectivity of catalysts P and S. Fractional conversions of butene into various products as a function of overall butene conversion. (a) Catalyst P. (b) Catalyst S. (●) Octanes. (○) TMP. (□) DMH. (▲) Light products. (◆) Heavy products.

Table 2
Alkylation over catalysts P and S at 273 K: distribution (%) of the octane isomers at two times on stream; comparison with zeolite HY

Catalyst/temperature	P (273 K)		S (273 K)		HY (353 K)
Time on stream (h)	1.6 (t_0)	6.3	1.3 (t_0)	7.5	1.7
Butene conversion (%)	78	4	85	7	75
C_8 in alkylate (wt.%)	44	75	41	85	55
TMP in C_8 (wt.%)	54	66	88	92	74
2,2,4-TMP	60	57	54	40	42
2,2,3-TMP	4	< 1	15	15	17
2,3,4-TMP	16	20	14	22	17
2,3,3-TMP	21	23	17	2	24
DMH in C_8 (wt.%)	44	29	12	8	20
2,2- + 3,3-DMH	23	< 3	14	< 3	< 1
2,4- + 2,5-DMH	64	86	74	> 90	48
2,3-DMH	6	7	12	< 3	43
3,4-DMH	9	7	< 2	< 3	8
M C_7 in C_8 (wt.%)	2	6	< 2	1	6

The curves of Fig. 4 show that, over both Al$_2$O$_3$–Cl catalysts, the yield of TMP goes through a maximum at about 70% overall conversion, whereas the yields of DMH as well as light and heavy products steadily increase with conversion. Thus, numerous secondary or side reactions tend to limit the yield of TMP.

With both catalysts, the DMH contain a vast majority of 2,4- and 2,5-isomers, some 2,2- and 3,3- and very little 3,4-isomer (Table 2). The DMH are commonly ascribed to the dimerization of *n*-butene via an intermediate 3,4-DMH$^+$ ion, which may then isomerize into other DMH$^+$ and then desorb as alkanes [4]. However, the decrease of the DMH/TMP ratio with the decline in activity over catalyst P, as well as the absence of the 3,4-DMH over catalyst S, suggest that the DMH largely arise from isomerization of the TMP$^+$ ions produced in step (a). Although isomerization of TMP into DMH is rather difficult at 273 K, it readily occurs in H$_2$SO$_4$ medium [24], and direct evidence for this process was obtained with the Al$_2$O$_3$–Cl catalysts [25]. The relative importance of the two mechanisms, dimerization or isomerization of TMP, cannot be assessed.

Cracking is obviously the main factor that limits the yield of TMP, notably with catalyst S. Among the cracked products, more isopentane was observed in the initial period over catalyst

S (64% of the light fraction) than over P (56%), and accordingly, less heptanes. Then, the proportion of isopentane decreased as conversion declined on both catalysts, so that at an intermediate TOS, catalyst P gave a higher yield of isopentane (Table 3).

The distributions among the C$_6$ and C$_7$ isomers were rather stable over catalyst S, whereas they changed markedly with TOS over P. With catalyst S, the main hexane was 2,3-dimethylbutane (2,3-DMB) followed by 2-methylpentane (2-MP), while the main heptane was 2,4-dimethylpentane (2,4-DMP), with less 2,3-DMP

Table 3
Alkylation over catalysts P and S at 273 K: composition (wt.%) of the light products C$_5$–C$_7$ at an intermediate time on stream

Catalyst	P	S
Time on stream (h)	4.7	3.6
Butene conversion (%)	18	18
C$_5$–C$_7$ in alkylate (wt.%)	19	22
Isopentane	52	40
Hexanes	24	32
2,3-DMB	49	55
2,2-DMB	6	9
2-MP	32	27
3-MP	13	9
Heptanes	24	28
2,4-DMP	65	61
2,3-DMP	16	19
2-MH	10	9
3-MH	9	4

(Table 3). A similar repartition was found with the aged catalyst P. However, the fresh P gave a repartition closer to thermodynamics, with much less 2,3-DMB among the C_6 and 40% of methylhexanes among the C_7. Again, alkane isomerization runs faster with catalyst P.

Alkanes C_5 to C_7 as well as the C_9–C_{11} arise from the cracking of heavy carbenium ions such as C_{12}^+ or C_{16}^+, which appear when the TMP^+ cations undergo further alkylation by n-butene:

$$TMP^+ + C_4H_8 \rightarrow C_{12}H_{25}^+ \quad (b);$$

then

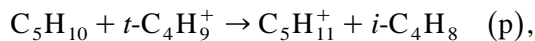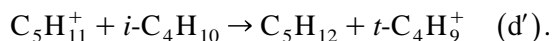$$C_{12}^+ + C_4H_8 \rightarrow C_{16}^+.$$
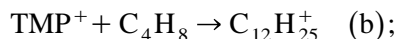
A striking feature of the reaction over Al_2O_3–Cl is the absence of alkenes at any stage, notably in the cracked products. Consider for instance the cracking of C_{12}^+:

$$C_{12}^+ \rightarrow C_5H_{10} + C_7^+ \quad (\text{or } C_6H_{12} + C_6^+).$$
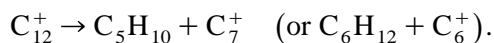
The C_7^+ carbenium ion readily desorbs as dimethylpentane upon hydride transfer as in step (d). However, the alkene C_5H_{10} is transformed into isopentane by successive transfers of H^+ and then H^-. The proton donor may be a t-butyl cation:

$$C_5H_{10} + t\text{-}C_4H_9^+ \rightarrow C_5H_{11}^+ + i\text{-}C_4H_8 \quad (p),$$

then

$$C_5H_{11}^+ + i\text{-}C_4H_{10} \rightarrow C_5H_{12} + t\text{-}C_4H_9^+ \quad (d').$$

If this occurs, the isobutene rapidly condenses with a t-butyl$^+$ to give a TMP^+ cation (self-alkylation). This would result in a yield of TMP higher than actually observed over the fresh catalysts. Destructive alkylation [26] is a more plausible mechanism, since in that case, the proton transferred to the adsorbed alkene is provided by a C_8^+ carbenium ion:

$$TMP^+ \text{ (or } DMH^+) + C_5H_{10} \rightarrow TMPentene$$

$$\text{(or DMHexene)} + C_5H_{11}^+ \quad (p'),$$
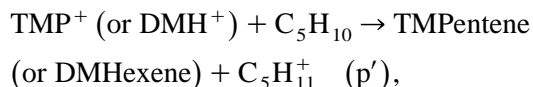
the $C_5H_{11}^+$ ion being desorbed as isopentane (step d'). The intermediate octene readily condenses with a t-butyl carbenium ion to regenerate a C_{12}^+.

Similarly, the appearance of C_9 and heavier alkanes is explained by the cracking of heavier ions such as C_{16}^+. As the surface is permanently covered with various branched alkenes, these may condense with the C_4^+ or C_8^+, giving branched carbenium ions of intermediate size, which in turn participate to the cracking sequence. Propene probably reacts in this way, since propane was never detected. Indeed, it has been proposed that only tertiary carbenium is able to desorb [22]. In any case, one isobutane unit incorporates in every alkane molecule, and the partial yields appearing in Fig. 4 were calculated in this way.

As with other solid catalysts [27], the rate of cracking does not exactly balance the rate of growth of the heavier species, and the carbonaceous deposit that builds up on the surface results in a rapid activity decay. Although the various products arise from primary as well as secondary reactions, the lower cracking and higher selectivity for octanes observed upon aging of catalyst Al_2O_3–Cl clearly cannot be due to the loss in conversion only. Thus, the various catalytic steps are not affected in the same way, those involving successively condensation and cracking followed by proton transfer (p or p') being more rapidly poisoned than hydride transfers.

3.1.5. Influence of reaction conditions

The Al_2O_3–Cl catalysts were tested at several temperatures between 263 and 353 K, under the same flow conditions as above. With catalyst S, for instance, the initial conversion amounted to 60% at 263 K, 88% at 313 K and 53% at 353 K.

The reaction at 263 K featured the best selectivity. Initially, the alkylate contained 85% octanes (of which 98% were TMP) and about 10% light products, then the composition did not change much upon aging. But with the rise in temperature, increasing amounts of cracked products were found at TOS = t_0, and less and less TMP among the C_8. Then the alkylate

composition changed with TOS in the same way as at 273 K, except at 353 K where the proportion of TMP decreased at the benefit of the DMH and methyl-heptanes.

However, catalyst S deactivated at all temperatures, the lifetime varying as:

273 K ≫ 263 K > 313 K, 353 K.

Therefore, operation at 273 K afforded by far the highest durability. A similar result was found with catalyst P.

Then the dilution isobutane–butene was raised from 20 to 50 at constant butene flow rate over catalyst P at 273 K. The amount of light products was divided by two and the selectivity to TMP was improved by 20%. Surprisingly, the catalyst deactivated faster than at dilution 20. Best results were obtained when the butene flow rate was reduced to 0.17 g h^{-1} g^{-1} at dilution 50: the conversion of butene exceeded 95% for the first 5 h, then slowly decreased to 40% after 15 h, but ultimately went to zero.

3.1.6. Comparison of Al_2O_3–Cl with zeolite Y

The Al_2O_3–Cl catalysts were compared with a zeolite HY (LZY 82), previously dehydrated at 773 K. As the zeolite operates preferably above 323 K [22], the test was carried out at 353 K, using the same dilution (20) and flow rate as above.

Results are shown on Fig. 5. The conversion of butene at time t_0 was 75%, slightly under that with solid P at 273 K, and steadily decreased to 45% during the first 5 h on stream, but from then on it remained rather stable for the next 15 h (Fig. 5a). The product pattern differed somewhat from that over Al_2O_3–Cl. Initially, the zeolite gave less cracked products (33% vs. 50%) but more C_8 (54% vs. 44%) and more heavy products (13% vs. 6%). The C_8 were made of 58% TMP, 40% DMH, and about 2% octenes. After 6 h on stream, the light products C_5–C_7 had vanished, and the heavy products rose to 35% (Fig. 5b). Meanwhile, the TMP fell down to nearly zero, and octenes appeared in increasing amounts so that after 10 h, the C_8 fraction contained mainly dimethyl-hexenes. The final carbon contents established at 9% for the zeolite, instead of 1.5% for Al_2O_3–Cl.

Thus, chlorinated alumina appears more active than zeolite HY in view of the lower reaction temperature, and its higher level of cracking is probably due to a stronger acidity. On both types of catalysts, the acid sites are rapidly blocked by strongly held species, but the zeolite retains activity for a longer time than Al_2O_3–Cl, although its selectivity progressively shifted from alkylation towards dimerization. The C_8^+ carbenium ions can still desorb from the zeolite
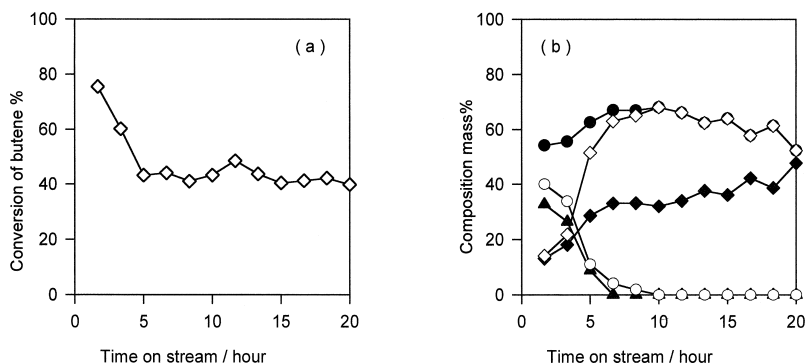

Fig. 5. Alkylation of isobutane with butene as a function of time on stream over zeolite HY at 353 K. Dilution $\alpha = 20$ mol mol^{-1}. Alkene mass flow rate 0.35 g g^{-1} h^{-1}. (a) Conversion of butene (◇). (b) Composition of the alkylate (mass%). (▲) Light products. (◆) Heavy products. (●) Octanes + octenes. (○) TMP. (◇) Others C_8.

as alkenes, thus restoring some protonic sites. By contrast, desorption of the TMP and other alkanes from Al_2O_3–Cl relies only on hydride transfer, which is quickly poisoned, and oligomerization is relatively unimportant. It then seems that alkenes cannot be desorbed from the chlorinated surface when isobutane is present, so that the acid sites are not renewed under reaction conditions. Thus, rejuvenation of the catalyst appears necessary.

3.2. The role of adsorbed HCl

3.2.1. Chlorinating procedure

The alkylation with butene over Al_2O_3–Cl proceeds only when the surface has been reacted with HCl, and thus features Brønsted acidity. A number of processes concur with alkylation, and form strongly adsorbed products which deactivate the catalyst. However, the decay is not immediate as it was for catalyst G.

The two-steps (S) and particularly the single step treatment (P at 940 K) require a sizeable activation energy and they likely result in hydrogen chloride bound to the surface. Nevertheless, the chlorinated catalysts are fragile since, in agreement with Myers [17], it appeared necessary to cool them under flowing HCl. As an example, when catalyst S was further swept with N_2 at 423 K prior to the alkylation test, and then cooled under N_2, the conversion of butene measured at time t_0 was 17% only.

Thus, some HCl weakly bound to the surface are involved in the reaction site. Accordingly, the desorption of HCl was investigated by means of TPD.

3.2.2. TPD results

Prior to the TPD, the various Al_2O_3–Cl samples were flushed with nitrogen in the same way as for the catalytic test, i.e., at 573 K for catalyst G, or 353 K for catalysts P and S. Then no $AlCl_3$ was released from any of the solids during the TPD. The only gas evolved was identified as HCl in several ways, including infrared (IR) spectroscopy. Starting the TPD at 323 K, the total amounts of HCl recovered at any temperature were recorded, and the final quantities measured at 973 K agreed well with the difference in Cl contents determined by chemical analyses of the solids (Table 4). Thermograms of the three catalysts are plotted on Fig. 6 in a differential form.

Desorption of HCl started at temperatures as low as 350 K for catalysts P and S. In the low temperature region, solid P released more HCl than S, but its rate of desorption slowly decreased above 400 K, whereas an acceleration was noted for catalyst S near 550 K. The HCl evolved at 593 K represented 16% of the total Cl content in catalyst P and 12% in S (Table 4). Then elution from solid S became more important, with a broad maximum in rate near 600 K.

Table 4
TPD and IR data for Al_2O_3–Cl catalysts: chlorine contents and amounts of HCl desorbed (μmol g^{-1}); IR band intensities of adsorbed pyridine (Lewis) and lutidine (Brønsted)

Catalyst	G	P	S
Total Cl (μmol g^{-1})	1637	1337	1840
HCl desorbed by TPD (μmol g^{-1})			
At 593 K	12	220	220
At 973 K	298	454	605
Residual Cl (μmol g^{-1})	1357	877	1250
IR band intensities (from Ref. [16])			
Pyridine (L sites, μmol g^{-1})[a]	220	180	110
Lutidine (B sites, au)[b]	15	230	405

[a]Band at 1625 cm^{-1} recorded after evacuation of excess base at 423 K.
[b]Band at 1645–1655 cm^{-1} recorded after evacuation of excess base at 298 K.

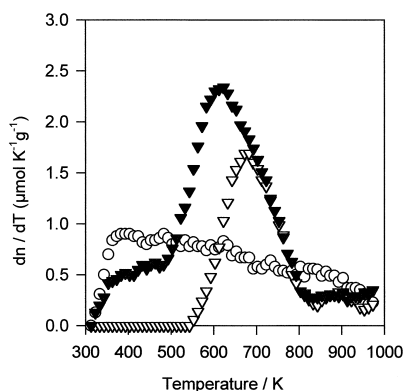Fig. 6. TPD of Al_2O_3–Cl catalysts. Rate of removal of HCl (μmol K^{-1} g^{-1}) vs. temperature. He flow: 25 cm^3 min^{-1}. Heating rate: 2.5 K min^{-1}. (○) Catalyst P. (▽) Catalyst G. (▼) Catalyst S.

Elution of HCl from catalyst G started at 550 K, so that 0.7% only of the total chlorine had been released at 593 K. An important desorption occurred above 600 K, with a maximum in rate at 670 K. At the final temperature (973 K), catalyst G had lost 18% of its chlorine content, against 34% for P and 32% for S.

The wide range of desorption temperatures suggests that a variety of desorption energies are involved on each catalyst. These were estimated by fitting the elution curves with an appropriate distribution of sites. The calculation used standard values of the adsorption and desorption rate constants [28]. For catalyst G, a majority of sites with energies between 160 and 180 kJ mol^{-1} could reproduce the curve up to 800 K. A few sites (10% of the total) with energies up to 250 kJ mol^{-1} have to be introduced to account for the region above 850 K. For catalysts P and S, the lower energy limit is more uncertain. A distribution of sites between 80 and 160 kJ mol^{-1} plausibly accounts for the desorption recorded under 650 K, and a few sites with energies above 160 kJ mol^{-1} fit the high temperature region.

3.3. Discussion

Desorption measurements show that various forms of adsorbed HCl occur at the surface of

Al_2O_3–Cl catalysts. These are to be related with IR and catalytic data.

Only those catalysts that were found active in alkylation, i.e., solids P and S, can release about 220 μmol HCl/g under 600 K. Furthermore, IR experiments [16] showed that catalysts P and S contacted with pyridine or lutidine featured both Brønsted and Lewis acidity, whereas Lewis sites only were detected over catalyst G prepared with CCl_4 (Table 4). Therefore, the activity in alkylation seems to be related with the Brønsted acidity brought about by weakly bound HCl, i.e., desorbing under 550 K.

Yet in a nuclear magnetic resonance (NMR) study, Sang et al. [29] detected Brønsted acid sites on a catalyst that had been prepared by reacting alumina with CCl_4 or $CHCl_3$. Substitution of the hydroxyls of alumina by chloride ions produces water and hydrogen chloride, which remain largely adsorbed when the solid is cooled under the chlorinating mixture. By contrast, sweeping catalyst G under nitrogen at 573 K, as was done in this study, likely desorbed most of the weakly bound HCl and water, as no HCl was eluted from the solid under 550 K.

Hydrogen chloride may be bound to the surface of Al_2O_3–Cl in a number of ways. Over the HCl-treated catalysts P and S, IR detected hydroxyl vibrations, and the large shift in ν_{OH} was attributed to hydrogen bonding, presumably with physisorbed HCl molecules [16]. Physisorption occurs when the solid is cooled in the presence of gaseous HCl, and the molecules bound in this way are expected to be fully desorbed at about 500 K. The TPD data suggest that the physisorbed species are more abundant on catalyst P than on S.
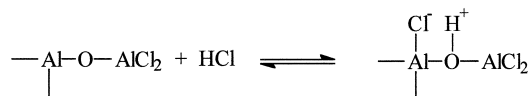
Furthermore, the HCl molecule may also be chemisorbed on a Lewis site of the chlorinated surface. When the surface is first reacted with CCl_4 and thus possesses strong Lewis acid sites, chemisorption does not occur under 373 K as this was the lowest temperature to obtain an active S catalyst. In the one-step treatment with HCl, the chemisorption of HCl follows the creation of the Lewis sites, which occurs at higher

temperature. In the literature, chemisorption has been pictured:

(i) either without dissociation [30]:

$$-Al-O-AlCl_2 + HCl \rightleftharpoons -Al-O-AlCl_3^- \ H^+$$
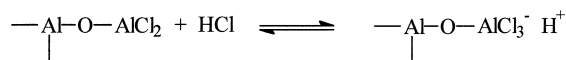
(ii) or with dissociation [20]:

$$-Al-O-AlCl_2 + HCl \rightleftharpoons -\overset{\overset{\displaystyle Cl^- \ H^+}{|}}{\underset{|}{Al}}-O-AlCl_2$$

There may be a variety of such chemisorbed species, depending on the coordination of the surface aluminium ions [30], and also on the mode of chlorination. In a previous IR study, the relative intensities of the band of protonated lutidine indicated that more Brønsted sites occurred over catalyst P than over S [16]. This result is in apparent contradiction with the TPD data, but both sets of results may be reconciled if the Brønsted sites detected by IR correspond only to a fraction of the HCl which is desorbed between 513 and 653 K. Moreover, the residual water content may be another factor influencing the adsorption (and desorption) of HCl. The peculiar behavior of the catalyst reacted with $HCl + H_2$ at 923 K is tentatively assigned to a water content lower than for the solids treated at 548 K, which modifies the interaction between HCl and the surface.

Finally, all catalysts lose more HCl between 700 and 973 K, as the total release stands between 300 μmol g^{-1} (catalyst G) and 600 μmol g^{-1} (catalyst S). Such values exceed the estimated numbers of hydroxyls left on catalysts P and particularly S, where the surface is apparently devoid of protons. The loss of HCl may then be ascribed to the recombination of surface chloride ions with protons occurring underneath the surface, or even in the bulk of γ-alumina. Hence, desorption above 700 K would be an irreversible process, controlled by diffusion.

4. Conclusions

The behavior of chlorinated alumina as a catalyst for the isobutane–butene alkylation strongly depends on the preparation procedure. The Lewis catalysts obtained by treatment with $CCl_4 + N_2$ are immediately self-poisoned. The catalysts treated with HCl and featuring Brønsted acidity are active at 273 K but decay after a few hours. Contrary to a HY zeolite, their selectivity does not shift towards oligomerization.

The activity of the Brønsted-type Al_2O_3–Cl catalysts recalls that of other supported acids [9,10] and they may be termed 'supported HCl catalysts.' The very strong acidic sites which catalyze the alkylation with butene are tentatively associated with chemisorbed HCl, which may be desorbed under 550 K, but physisorbed HCl also seems necessary with respect to activity and catalyst lifetime. Unfortunately, the influence of each particular type of adsorbed HCl upon catalytic behavior could not be established more precisely as the plug flow reactor did not allow measurements of conversion in stable regime. A stirred reactor [27], where the local alkene concentration is kept low, would probably delay the formation of strongly adsorbed species, and thus improve the durability of the catalyst.

References

[1] L.F. Albright, Oil Gas J. (November 12, 1990) 79.
[2] L.F. Albright, Oil Gas J. (November 26, 1990) 70.
[3] L.F. Albright, K.E. Kranz, Ind. Eng. Chem. Res. 31 (1992) 475.
[4] A. Corma, A. Martinez, Catal. Rev. Sci. Eng. 35 (1993) 483.
[5] S. Unverricht, S. Ernst, J. Weitkamp, Zeolite and related

microporous materials: state of the art 1994, in: J. Weitkamp, H.G. Karge, H. Pfeifer, W. Hölderlich (Eds.), Stud. Surf. Sci. Catal., Elsevier, Amsterdam, Vol. 84, 1994, p. 1693.

[6] A. Corma, A. Martinez, C. Martinez, Catal. Lett. 28 (1994) 187.

[7] A. Corma, M.I. Juan-Rajadell, J.M. Lopez-Nieto, A. Martinez, C. Martinez, Appl. Catal. A 111 (1994) 175.

[8] T. Okuhara, M. Yamashita, K. Na, M. Misono, Chem. Lett. 8 (1994) 1451.

[9] S.I. Hommeltoft, H.F.A. Topsoe, Eur. Patent no. 0433954A1, June 1991, issued to Haldor Topsoe.

[10] J.F. Joly, E. Benazzi, C. Marcilly, Eur. Patent no. 059277A1, April 1993, issued to IFP.

[11] M.F. Simpson, J. Wei, S. Sundaresan, Ind. Eng. Chem. Res. 35 (1998) 3861.

[12] J.E. Child, T.S. Tchou, A. Huss, C.R. Kennedy, F.P. Ragonese, F.A. Tabak, US Patent no. 4956518, Sept. 1990, issued to Mobil.

[13] J.V. Fletcher, A.G. Goble, US Patent no. 3240840, 1966, issued to BP.

[14] US Patent no. 4113657, 1978, issued to Texaco.

[15] A.K. Roebuck, B.L. Evering, Ind. Eng. Chem. Prod. Res. Dev. 9 (1970) 76.

[16] G. Clet, J.M. Goupil, D. Cornet, Bull. Soc. Chim. France 134 (1997) 223.

[17] J.W. Myers, Ind. Eng. Chem. Prod. Res. Dev. 10 (1971) 200.

[18] J.M. Goupil, J.L. Poirier, D. Cornet, Catal. Lett. 31 (1995) 121.

[19] D. Cornet, J.M. Goupil, G. Szabo, J.L. Poirier, G. Clet, Appl. Catal. A 141 (1996) 193.

[20] A. Kytökivi, M. Lindblad, A. Root, J. Chem. Soc. Faraday Trans. 91 (1995) 941.

[21] A. Corma, A. Martinez, C. Martinez, J. Catal. 146 (1994) 185.

[22] F. Cardona, N.S. Gnep, M. Guisnet, G. Szabo, P. Nascimento, Appl. Catal. A 128 (1995) 243.

[23] P.M. Bernard, M. Primet, J. Chem. Soc. Faraday Trans. 86 (1990) 567.

[24] D.J. am Ende, L.F. Albright, Ind. Eng. Chem. Res. 33 (1994) 840.

[25] G. Clet, Thesis, University of Caen, 1997.

[26] L. Schmerling, in: G.A. Olah (Ed.), Friedel-Crafts and Related Reactions, Interscience Publishers, New York, Vol. 2, Part 2, 1964, p. 1075.

[27] G.S. Nivarty, K. Seshan, J.A. Lercher, Microporous and Mesoporous Materials 22 (1998) 379.

[28] S.B. Sharma, B.L. Meyers, D.T. Chen, J. Miller, J.A. Dumesic, Appl. Catal. A. 102 (1993) 253.

[29] H. Sang, H.Y. Chu, J.H. Lunsford, Catal. Lett. 26 (1994) 235.

[30] J. Thompson, G. Webb, J.M. Winfield, J. Mol. Catal. 68 (1991) 117.